Hindawi Publishing Corporation
Journal of Applied Mathematics
Volume 2014, Article ID 539459, 7 pages
http://dx.doi.org/10.1155/2014/539459

Research Article

The Burgers Equation for a New Continuum Model with Consideration of Driver's Forecast Effect

Lei Yu[1] and Bingchang Zhou[2]

[1] *College of Automation, Northwestern Polytechnical University, Xi'an, Shaanxi 710129, China*
[2] *School of Science, Northwestern Polytechnical University, Xi'an, Shaanxi 710129, China*

Correspondence should be addressed to Lei Yu; yuleijk@126.com

Received 18 June 2014; Revised 12 August 2014; Accepted 12 August 2014; Published 24 August 2014

Academic Editor: Weichao Sun

A new continuum model with consideration of driver's forecast effect is obtained to study the density wave problem and the stop-and-go phenomena. The stability condition of the new model is derived by using linear analysis. The triangular shock wave, one type of density wave, which is determined by Burgers equation in the stable region, is discussed in great detail with reductive perturbation method. The local cluster appears when we perform the numerical simulations for the new model. It also proves that the driver's forecast effect has the positive effect of reducing the local cluster.

1. Introduction

Traffic jams, the typical signature of the complex behavior of vehicular traffic, have been studied by various traffic models [1–8]. From different theoretical basis, there are microscopic and macroscopic models to describe traffic flow. The dynamical aspects of microscopic models are based on the description of the individual vehicles' situation. This process is largely determined by the drivers' behavior and the physical performance of vehicles. The macroscopic models describe traffic streams as a compressible fluid obeying global rules. This coarse-grained means is needed for understanding the collective behavior of traffic, designing efficient control strategies, developing macroscopic traffic simulation, and so forth.

Bando et al. [9] propose the optimal velocity (OV) model to characterize the car-following behavior. Although the OV model is shown to have the universal structure in describing many properties of traffic flow, many approaches to extending the model toward more realistic traffic model have been pursued. Helbing and Tilch [10] develop a generalized force model with a velocity difference term added into the OV model. Xue et al. [11] extend the OV model to take into account the effect of the relative velocity.

The pioneer work of continuum traffic flow models is the LWR model [12, 13]. Although the LWR model can reproduce most basic traffic flow phenomena such as traffic congestion formation and dissipation in heavy traffic, this model can not describe nonequilibrium traffic flow dynamics and does not have the ability to explain the amplification of small disturbances in heavy traffic. To overcome the deficiencies in the LWR model, various macroscopic traffic models have been proposed. Payne [14] introduces a high-order continuum model which can describe the amplification of small disturbances in heavy traffic and allow fluctuations of speed around the equilibrium value. Thus, the Payne model is suitable to describe nonequilibrium situations such as stop-and-go traffic. However, a fundamental principle of traffic flow, that is, a car being influenced only by the motion of cars ahead of it, not by the motion of cars behind it, is violated in the Payne model because one characteristic speed of this model is greater than the macroscopic flow speed. Notice that cars are anisotropic particles and respond only to frontal stimuli. Jiang et al. [15] develop a macroscopic continuum model based on a car-following theory. This model overcomes the characteristic speed problem that exists in many high-order continuum models such as the Payne model.

However, the consistency between microscopic and macroscopic models has been proved [16]. There are also some papers to derive macroscopic continuum models from micromodels (mainly the car-following models), such as [14, 15, 17].

There are many studies to reveal nonlinear phenomena of vehicular traffic, such as stop-and-go, phase transition, self-organized, and the nonlinear waves. Kurtze and Hong [18] derive the Korteweg-de Vries (KdV) equation from one continuum traffic flow model. Zhou et al. [19] obtain the KdV equation and the modified Korteweg-de Vries (mKdV) equation from the continuum traffic flow model derived from a car-following model. Ou [17] obtains the Burgers equation and the KdV equation from a continuum version of the full velocity difference car-following model. Yu et al. [20] investigate density waves in an optimal velocity model with reaction-time delay of drivers and derive the Burgers, KdV, and mKdV equations. However, the nonlinear waves results of the continuum traffic flow models are far less than those of the car-following models. The reason is probably the complex partial differential forms of the continuum traffic flow models.

In fact, the future traffic situation can be forecasted by the intelligent transportation system (ITS) based on the current traffic status, so the driver may be guided by the forecast information to adjust his/her current acceleration. However, few models consider the drivers forecast effect. Recently, a new car-following model with the driver's forecast effect is proposed by Tang et al. [21]. Similar to the other models which consider the information of ITS, the model presented by Tang et al. [21] can improve the stability of traffic flow and reduce traffic jams.

In this paper, a new macroversion is obtained based on the anisotropic continuum model proposed by Tang et al. [21]. The density wave problem and the stop-and-go phenomena are studied. In Section 2, the stability condition of the model is derived. In Section 3, the triangular shock wave, which is determined by the Burgers equation in the stable region, is discussed in great detail by using nonlinear analysis. In Section 4, the simulation results are given. These results prove that the driver's forecast effect has the positive effect of reducing the local cluster. Finally, a summary is given.

2. The Model and Its Stability Analysis

The new car-following model with the consideration of the driver's forecast effect can be written as follows [21]:

$$\begin{aligned}\frac{\mathrm{d}v_n(t)}{\mathrm{d}t} &= \kappa\left(V\left(\Delta x_n(t)\right) - v_n(t)\right)\\ &\quad + \beta\kappa\left(V\left(\Delta x_n(t+\tau)\right) - v_n(t+\tau)\right),\end{aligned} \tag{1}$$

where κ is the reactive coefficient, β is the coefficient of the driver's forecast effect, and τ is the time-step of the driver forecast. Using the transformation between microvariables and macrovariables, the corresponding anisotropic macro-continuum model of (1) is obtained [21], that is, the following equations:

$$\begin{aligned}&\frac{\partial\rho}{\partial t} + \frac{\partial(\rho v)}{\partial x} = 0,\\ &\frac{\partial v}{\partial t} + v\frac{\partial v}{\partial x} = \frac{(1+\beta)\left(V_e(\rho) - v\right)}{T+\beta\tau} + \beta\tau u_e'(h)\, c_0\frac{\partial v}{\partial x},\end{aligned} \tag{2}$$

where T is the reactive time given by the inverse of the coefficient κ, $c_0 = \epsilon/(\beta\tau+T) > 0$ is the propagating velocity of the small perturbation, ϵ is the distance between the following and leading vehicles in micromodel, and

$$u_e(h) = V_e(\rho), \quad h = 1/\rho. \tag{3}$$

To derive the stability condition, the Burgers equation, and its shock solution of the macroversion of (1), the following new macromodel is derived from (2) according to (3); that is,

$$\begin{aligned}&\frac{\partial\rho}{\partial t} + \frac{\partial(\rho v)}{\partial x} = 0,\\ &\frac{\partial v}{\partial t} + v\frac{\partial v}{\partial x} = \gamma\left(V_e(\rho) - v\right) - \beta\tau c_0\rho^2 V_e'(\rho)\frac{\partial v}{\partial x},\end{aligned} \tag{4}$$

where $\gamma = (1+\beta)/(T+\beta\tau)$. Obviously, model (4) is anisotropy.

The linear stability theory will be applied to derive the linear stability condition of model (4). Assume traffic to be initially in a state differing infinitesimally from the uniform steady flow. Similar to the decomposition of the flow of (4) into a linear combination of Fourier modes in [18], we have

$$\begin{aligned}\rho(x,t) &= \rho_0 + \sum_k \widehat{\rho}_k \exp\left(ikx + \sigma_k t\right),\\ v(x,t) &= v_0 + \sum_k \widehat{v}_k \exp\left(ikx + \sigma_k t\right),\end{aligned} \tag{5}$$

where ρ_0 and v_0 are the uniform steady states of (4). Substituting (5) into (4), linearizing and neglecting the higher-order terms of the small perturbations $\widehat{\rho}_k$ and $\widehat{v}_k$, we have

$$\left(\sigma_k + ikv_0\right)\widehat{\rho}_k + ik\rho_0\widehat{v}_k = 0, \tag{6}$$

$$\begin{aligned}\sigma_k\widehat{v}_k + ikv_0\widehat{v}_k &= \gamma\left(V_e'(\rho_0)\,\widehat{\rho}_k - \widehat{v}_k\right)\\ &\quad - \beta\tau c_0\rho_0^2 V_e'(\rho_0)\, ik\widehat{v}_k.\end{aligned} \tag{7}$$

From (6), we have

$$\widehat{\rho}_k = -\frac{ik\rho_0\widehat{v}_k}{\sigma_k + ikv_0}. \tag{8}$$

Substituting (8) into (7), the following quadratic equation is obtained:

$$\begin{aligned}&\left(\sigma_k + ikv_0\right)^2 + \left(\gamma + \beta\tau c_0\rho_0^2 V_e'(\rho_0)\, ik\right)\left(\sigma_k + ikv_0\right)\\ &\quad + \gamma\rho_0 V_e'(\rho_0)\, ik = 0.\end{aligned} \tag{9}$$

Consider the long wave expansion of σ_k in (9), which is determined order by order around $ik \approx 0$ [8]. By expanding $\sigma_k = \sigma_1(ik) + \sigma_2(ik)^2 + \cdots$ and separating the real part and the imaginary part, the coefficients of ik and $(ik)^2$ are derived as follows:

$$\begin{aligned} \sigma_1 &= -v_0 - \rho_0 V_e'(\rho_0), \\ \sigma_2 &= \frac{1}{\gamma}\rho_0^2 V_e'^2(\rho_0)(\varpi\rho_0 - 1), \end{aligned} \tag{10}$$

where $\varpi = \beta\tau c_0$.

The linear stability condition of (4) is decided by the real part of σ_k. In fact, the uniform traffic flow described by (4) is stable against all infinitesimal disturbances when $\sigma_2 > 0$; that is,

$$\varpi\rho_0 > 1. \tag{11}$$

It means that the traffic flow described by (4) is stable when (11) holds.

3. Nonlinear Analysis

To investigate the system behavior in the stable region, we consider the long wavelength modes on coarse-grained scales. The reductive perturbation method as in [8] is applied to (4). Introduce the slow scales for space variable x and time variable t and define slow variables X and T as follows:

$$X = \varepsilon(x - bt), \qquad T = \varepsilon^2 t, \tag{12}$$

where b is a constant to be determined and $0 < \varepsilon \ll 1$. We set the density and velocity as

$$\begin{aligned} \rho(x,t) &= \rho_0 + \varepsilon\widehat{\rho}(X,T), \\ v(x,t) &= v_0 + \varepsilon\widehat{v}(X,T). \end{aligned} \tag{13}$$

Substituting (12) and (13) into (4) and making the Taylor expansions to ε^3, the following nonlinear partial differential equations are derived:

$$\begin{aligned} &\varepsilon^2\left(\rho_0\partial_X\widehat{v} + v_0\partial_X\widehat{\rho} - b\partial_X\widehat{\rho}\right) \\ &\quad + \varepsilon^3\left(\partial_T\widehat{\rho} + \widehat{\rho}\partial_X\widehat{v} + \widehat{v}\partial_X\widehat{\rho}\right) = 0, \end{aligned} \tag{14}$$

$$\begin{aligned} &\varepsilon\gamma\left(\widehat{v} - V_e'(\rho_0)\widehat{\rho}\right) \\ &\quad + \varepsilon^2\left[\widehat{\rho}\widehat{v} + \left(v_0 - b + \varpi\rho_0^2 V_e'(\rho_0)\right)\partial_X\widehat{v}\right. \\ &\qquad \left. - V_e'(\rho_0)\widehat{\rho}^2 - \frac{1}{2}\gamma V_e''(\rho_0)\widehat{\rho}^2\right] \\ &\quad + \varepsilon^3\left[\partial_T\widehat{v} + \widehat{v}\partial_X\widehat{v} - \frac{1}{6}\gamma V_e'''(\rho_0)\widehat{\rho}^3\right. \\ &\qquad \left. + \left(\varpi\rho_0^2 V_e''(\rho_0) + 2\varpi\rho_0 V_e'(\rho_0)\right)\widehat{\rho}\partial_X\widehat{v}\right] = 0. \end{aligned} \tag{15}$$

From the coefficient of ε in (15), we have

$$\widehat{v} = V_e'(\rho_0)\widehat{\rho} + O\left(\varepsilon^2\right). \tag{16}$$

The relationship between the perturbation of density and velocity is given by (16) which is the basis of Burgers equation's derivation. According to (16), we have the value of b from the second term of ε in (14); that is,

$$b = \rho_0 V_e'(\rho_0) + v_0. \tag{17}$$

Then we have

$$\begin{aligned} \widehat{q} = \widehat{\rho}\widehat{v} &= \left(V_e'(\rho_0) + \frac{1}{2}\gamma V_e''(\rho_0)\right)\widehat{\rho}^2 \\ &\quad + \left(1 - \varpi\rho_0\right)\rho_0 V_e'^2(\rho_0)\partial_X\widehat{\rho}. \end{aligned} \tag{18}$$

Combining (14) and (18), the following equation is derived:

$$\begin{aligned} &\partial_T\widehat{\rho} + \left(2V_e'(\rho_0) + \gamma V_e''(\rho_0)\right)\widehat{\rho}\partial_X\widehat{\rho} \\ &\quad = \left(\varpi\rho_0 - 1\right)\rho_0 V_e'^2(\rho_0)\partial_X^2\widehat{\rho}. \end{aligned} \tag{19}$$

In accordance with stability condition (11), the coefficient of the second derivative term on the right hand side of (19) is positive in the stable region. Thus, in the stable region, (19) is just the Burgers equation.

If $\widehat{\rho}(X,0)$ is of compact support, the solution $\widehat{\rho}(X,T)$ of Burgers equation, (19), behaves like a train of N-triangular shock waves; that is,

$$\begin{aligned} \widehat{\rho}(X,T) &= \frac{1}{|c_1|T}\left(X - \frac{\eta_n + \eta_{n+1}}{2}\right) - \frac{\eta_{n+1} - \eta_n}{2|c_1|T} \\ &\quad * \tanh\left(\frac{c_2}{4|c_1|T}(\eta_{n+1} - \eta_n)(X - \xi_n)\right), \end{aligned} \tag{20}$$

where $c_1 = 2V_e'(\rho_0) + \gamma V_e''(\rho_0)$, $c_2 = (\varpi\rho_0 - 1)\rho_0 V_e'^2(\rho_0)$, ξ_n are the coordinates of the shock fronts, and η_n are the coordinates of the intersections of the slopes with the x-axis ($n = 1, 2, \ldots, N$). $\widehat{\rho}(X,T)$ decays to 0 like $O(1/T)$ when $T \to +\infty$. That is to say, any shock wave expressed by (19) in stable traffic flow region will evolve to a uniform flow in the course of time. We see this phenomenon in Figures 1(a) and 1(e) of Section 4.

4. The Numerical Simulation

To check the theoretical results, we carry out numerical simulations for model (4) by using the numerical scheme in [21]. The difference equations are as follows:

$$\rho_i^{j+1} = \rho_i^j + \frac{\Delta t}{\Delta x}\rho_i^j\left(v_i^j - v_{i+1}^j\right) + \frac{\Delta t}{\Delta x}v_i^j\left(\rho_{i-1}^j - \rho_i^j\right), \tag{21}$$

(a) if $v_i^j < -\varpi(\rho_i^j)^2 V_e'(\rho_i^j)$,

$$\begin{aligned} v_i^{j+1} &= v_i^j + \frac{\Delta t}{\Delta x}\left(-\varpi\left(\rho_i^j\right)^2 V_e'\left(\rho_i^j\right) - v_i^j\right)\left(v_{i+1}^j - v_i^j\right) \\ &\quad + \gamma\Delta t\left(V_e\left(\rho_i^j\right) - v_i^j\right), \end{aligned} \tag{22}$$

(b) if $v_i^j \geq -\varpi(\rho_i^j)^2 V_e'(\rho_i^j)$,

$$\begin{aligned} v_i^{j+1} &= v_i^j + \frac{\Delta t}{\Delta x}\left(-\varpi\left(\rho_i^j\right)^2 V_e'\left(\rho_i^j\right) - v_i^j\right)\left(v_i^j - v_{i-1}^j\right) \\ &\quad + \gamma\Delta t\left(V_e\left(\rho_i^j\right) - v_i^j\right), \end{aligned} \tag{23}$$

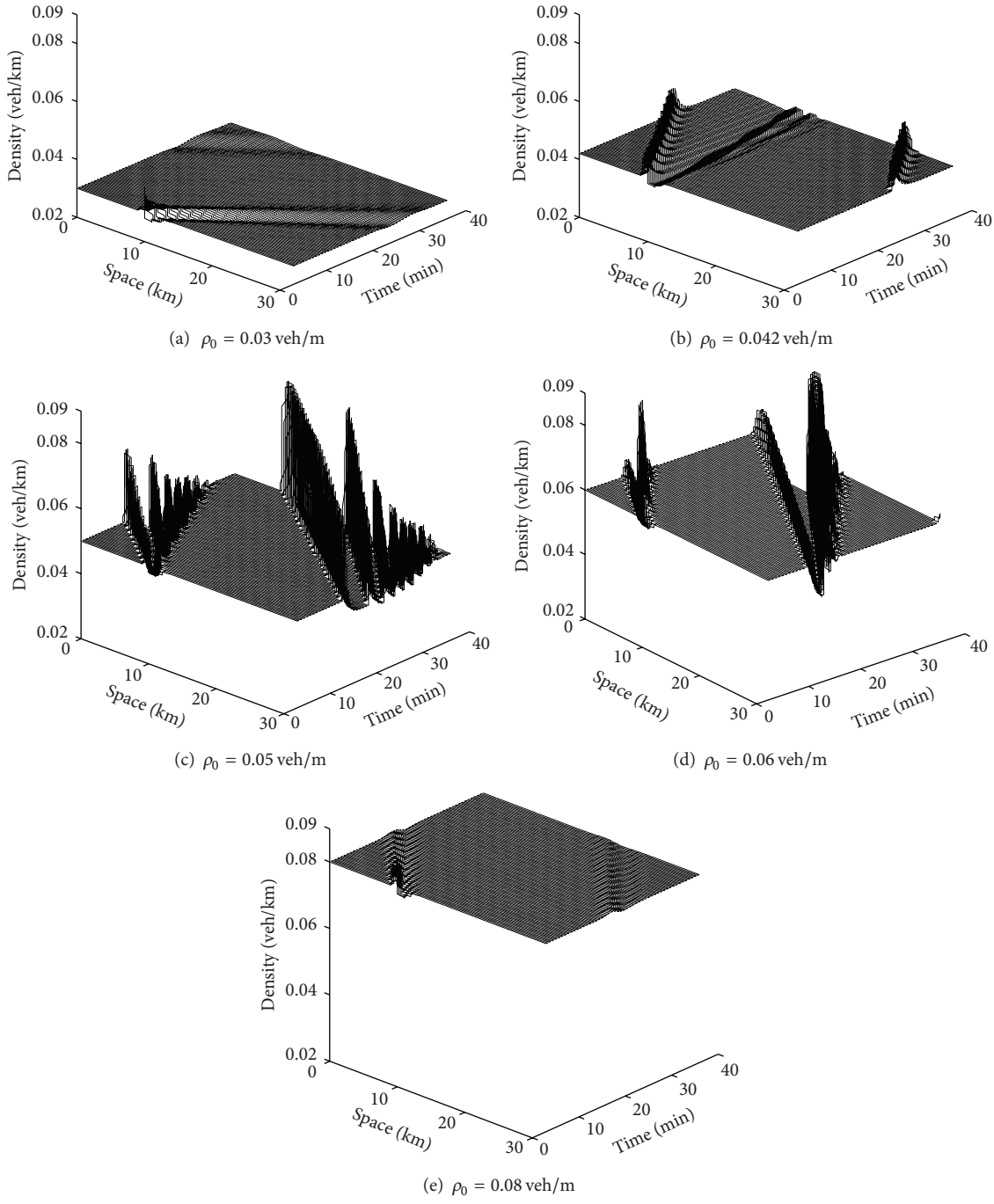

(a) $\rho_0 = 0.03$ veh/m

(b) $\rho_0 = 0.042$ veh/m

(c) $\rho_0 = 0.05$ veh/m

(d) $\rho_0 = 0.06$ veh/m

(e) $\rho_0 = 0.08$ veh/m

FIGURE 1: Temporal evolution of traffic flow before 40 minutes for different ρ_0 with $\beta = 0.2$.

where i, j, Δx, and Δt represent the road section, time, spatial step, and time step, respectively, $\rho_i^j \approx \rho(x_i, t_j)$, $v_i^j \approx v(x_i, t_j)$, $x_i = i\Delta x$, $t_j = j\Delta t$, and i, j are integers.

To study the local cluster effect of (4), we perform numerical simulations over a system of 32.2 km long highway using (21)–(23). The local cluster effect corresponds to the stop-and-go wave observed in the traffic flow due to the amplification of a small disturbance. We simulate the traffic flow under the periodic boundary conditions. The following variation of the initial density ρ_0 is used as in [15]:

$$\rho(x,0) = \rho_0 + \Delta\rho_0 \left\{ \cosh^{-2}\left[\frac{160}{L}\left(x - \frac{5L}{16}\right)\right] - \frac{1}{4}\cosh^{-2}\left[\frac{40}{L}\left(x - \frac{11L}{32}\right)\right]\right\}, \tag{24}$$

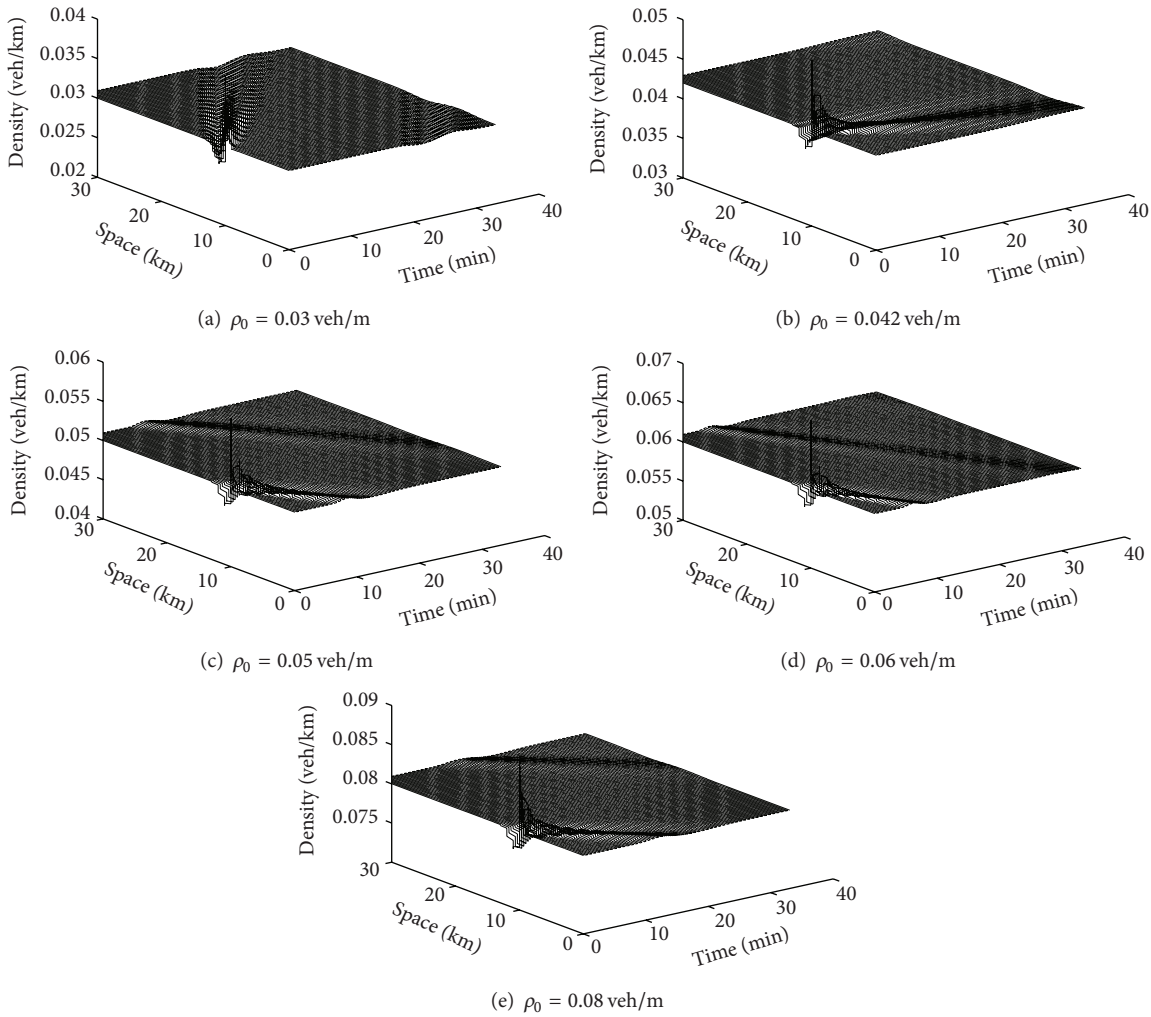

Figure 2: Temporal evolution of traffic flow before 40 minutes for different ρ_0 with $\beta = 0.4$.

where $L = 32.2$ km is the length of the road section under consideration. The periodic boundary conditions are given as follows:

$$\rho(L,t) = \rho(0,t), \qquad v(L,t) = v(0,t). \tag{25}$$

Here we use the equilibrium speed-density relationship proposed in [22]:

$$V_e(\rho) = v_f \left\{ \left[1 + \exp\left(\frac{\rho/\rho_m - 0.25}{0.06} \right) \right]^{-1} - 3.72 \times 10^{-6} \right\}. \tag{26}$$

Assume the initial flow to be in local steady state; that is, $v(x,0) = V_e(\rho(x,0))$. Let $\Delta\rho_0 = 0.01$ veh/m, let the space interval Δx be 100 m, and let the time interval Δt be 1 s. The choice of Δx and Δt satisfies the Courant-Friedrichs-Levy (CFL) stability condition. The other parameter values we take are as follows:

$$\begin{gathered} \tau = 5\,\text{s}, \qquad T = 10\,\text{s}, \qquad v_f = 30\,\text{m/s}, \\ c_0 = 11\,\text{m/s}, \qquad \rho_m = 0.2\,\text{veh/m}. \end{gathered} \tag{27}$$

Figures 1 and 2 show the evolution of initial uniform traffic flow under the small disturbance.

Figure 1 shows the temporal evolution of traffic flow before 40 minutes for different ρ_0 with $\beta = 0.2$. In pattern (a) of Figure 1, the initial density $\rho_0 = 0.03$ of traffic flow is so low that the disturbance dies out without any amplification with time. With the initial density ρ_0 increasing, small disturbance is amplified and so leads to the instability of traffic flow. The pattern (b) in Figure 1 shows that several local clusters form for the initial density $\rho_0 = 0.042$. In pattern (c) of Figure 1, the stop-and-go phenomenon, which is a complex local structure consisting of multiclusters, can be observed. Continuing to increase the initial density ρ_0, we can see a dipole-like structure which is illustrated by Figure 1(d). In pattern (e) of Figure 1, a stable traffic flow is reached again with the initial density $\rho_0 = 0.08$.

Figure 2 shows the temporal evolution of traffic flow before 40 minutes for different ρ_0 with $\beta = 0.4$. In patterns of Figure 2, there are no clusters and the disturbances propagate backward without any amplification with different initial densities ρ_0.

Comparing every subfigure of Figures 1 and 2, the value of β is the only different parameter. It is obvious that the increase of β leads to the stabilization of traffic flow. So the driver's forecast effect has the positive effect of reducing the local cluster. This result is coincident with the one in [21].

The above numerical results are not so perfect. The propagation speeds of the perturbation waves we get from our figures are about 40–60 km/h against the traffic direction, which are not very consistent with the ones from the real data. References [23, 24] point out that the propagation velocity which is obtained from the real data should be about −12–20 km/h. Many factors may lead to this result such as the option of equilibrium function, the difference scheme, or the parameters. The control and optimization problems of the parameters in our model can also be studied [25–30]. We will continue to study these problems in future.

5. Summary

In this paper, a new macroversion is proposed with the consideration of the driver's forecast effect proposed. The stability condition of the model is derived by using linear analysis. The triangular shock wave which is determined by Burgers equation in the stable region is discussed with reductive perturbation method. The stop-and-go phenomena appear when we carry out the numerical simulation for the model. The driver's forecast effect which has the positive effect of reducing the local cluster is proved.

Conflict of Interests

The authors declare that there is no conflict of interests regarding the publication of this paper.

Acknowledgments

This work is supported by National Natural Science Foundation of China (Grants nos. 11102155 and 11102165), Natural Science Foundation of Shaanxi Province (2013JQ7014 and 2012JM1001), the new direction of the Young Scholar of Northwestern Polytechnical University, and Foundation for Fundamental Research of Northwestern Polytechnical University (JC20110265).

References

[1] T. Ezaki and K. Nishinari, "Cluster size distribution in 1D-CA traffic models," *Journal of Physics A*, vol. 45, no. 4, Article ID 045101, 2012.

[2] W.-X. Zhu and R.-L. Yu, "Nonlinear analysis of traffic flow on a gradient highway," *Physica A: Statistical Mechanics and Its Applications*, vol. 391, no. 4, pp. 954–965, 2012.

[3] B. S. Kerner, "Physics of traffic gridlock in a city," *Physical Review E: Statistical, Nonlinear, and Soft Matter Physics*, vol. 84, Article ID 045102, 4 pages, 2011.

[4] X. M. Zhao, D. F. Xie, B. Jia, R. Jiang, and Z. Y. Gao, "Disorder structure of free-flow and global jams in the extended BML model," *Physics Letters A*, vol. 375, no. 7, pp. 1142–1147, 2011.

[5] D. Yang, J. Jin, B. Ran, Y. Pu, and F. Yang, "Modeling and analysis of car-truck heterogeneous traffic flow based on intelligent driver car-following model," in *Proceedings of the 92nd Annual Meeting on Transportation Research Board (TRB '13)*, Washington, Wash, USA, January 2013.

[6] T. Nagatani, "Jamming and freezing transitions in CA model for facing pedestrian traffic with a soft boundary," *Physics Letters A*, vol. 374, no. 15-16, pp. 1686–1689, 2010.

[7] S. Masukura, T. Nagatani, and K. Tanaka, "Jamming transitions induced by a slow vehicle in traffic flow on a multi-lane highway," *Journal of Statistical Mechanics: Theory and Experiment*, vol. 2009, no. 4, Article ID P04002, 2009.

[8] T. Nagatani, "The physics of traffic jams," *Reports on Progress in Physics*, vol. 65, no. 9, pp. 1331–1386, 2002.

[9] M. Bando, K. Hasebe, A. Nakayama, A. Shibata, and Y. Sugiyama, "Dynamical model of traffic congestion and numerical simulation," *Physical Review E*, vol. 51, no. 2, pp. 1035–1042, 1995.

[10] D. Helbing and B. Tilch, "Generalized force model of traffic dynamics," *Physical Review E*, vol. 58, no. 1, pp. 133–138, 1998.

[11] Y. Xue, L. Y. Dong, Y. W. Yuan, and S. Q. Dai, "The effect of the relative velocity on traffic flow," *Communications in Theoretical Physics*, vol. 38, no. 2, pp. 230–234, 2002.

[12] M. J. Lighthill and G. B. Whitham, "On kinematic waves: II. A theory of traffic flow on long crowed roads," *Proceedings of the Royal Society A*, vol. 229, no. 1178, pp. 317–345, 1955.

[13] P. I. Richards, "Shock waves on the highway," *Operations Research*, vol. 4, pp. 42–51, 1956.

[14] H. J. Payne, "Models of freeway traffic and control," in *Mathematical Models of Public Systems*, G. A. Bekey, Ed., vol. 1 of *Simulation Councils Proceedings Series*, pp. 51–61, 1971.

[15] R. Jiang, Q. Wu, and Z. Zhu, "A new continuum model for traffic flow and numerical tests," *Transportation Research Part B: Methodological*, vol. 36, no. 5, pp. 405–419, 2002.

[16] D. C. Gazis, R. Herman, and R. B. Potts, "Car-following theory of steady-state traffic flow," *Operations Research*, vol. 7, pp. 499–505, 1959.

[17] Z. Ou, "Density waves in the continuum analog of the full velocity difference model," *Physica A: Statistical Mechanics and its Applications*, vol. 387, no. 8-9, pp. 1799–1806, 2008.

[18] D. A. Kurtze and D. C. Hong, "Traffic jams, granular flow, and soliton selection," *Physical Review E*, vol. 52, no. 1, pp. 218–221, 1995.

[19] X. Zhou, Z. Liu, and J. Luo, "The density wave in a car-following model," *Journal of Physics A: Mathematical and General*, vol. 35, no. 20, pp. 4495–4500, 2002.

[20] L. Yu, T. Li, and Z. K. Shi, "Density waves in a traffic flow model with reaction-time delay," *Physica A*, vol. 389, no. 13, pp. 2607–2616, 2010.

[21] T. Q. Tang, H. J. Huang, and H. Y. Shang, "A new macro model for traffic flow with the consideration of the driver's forecast effect," *Physics Letters, Section A: General, Atomic and Solid State Physics*, vol. 374, no. 15-16, pp. 1668–1672, 2010.

[22] B. S. Kerner and P. Konhäuser, "Cluster effect in initially homogeneous traffic flow," *Physical Review E*, vol. 48, no. 4, pp. R2335–R2338, 1993.

[23] J. M. D. Castillo and F. G. Benítez, "On the functional form of the speed-density relationship-I: general theory," *Transportation Research Part B*, vol. 29, no. 5, pp. 373–389, 1995.

[24] B. S. Kerner, "Synchronized flow as a new traffic phase and related problems for traffic flow modelling," *Mathematical and Computer Modelling*, vol. 35, no. 5-6, pp. 481–508, 2002.

[25] W. C. Sun, H. J. Gao, and O. Kaynak, "Finite frequency H_∞ control for vehicle active suspension systems," *IEEE Transactions on Control Systems Technology*, vol. 19, no. 2, pp. 416–422, 2011.

[26] W. Sun, Z. Zhao, and H. Gao, "Saturated adaptive robust control for active suspension systems," *IEEE Transactions on Industrial Electronics*, vol. 60, no. 9, pp. 3889–3896, 2013.

[27] W. C. Sun, H. J. Gao, and O. Kaynak, "Adaptive backstepping control for active suspension systems with hard constraints," *IEEE/ASME Transactions on Mechatronics*, vol. 18, no. 3, pp. 1072–1079, 2013.

[28] G. D. Tian, M. C. Zhou, J. W. Chu, and Y. M. Liu, "Probability evaluation models of product disassembly cost subject to random removal time and different removal labor cost," *IEEE Transactions on Automation Science and Engineering*, vol. 9, no. 2, pp. 288–295, 2012.

[29] G. Tian, J. Chu, Y. Liu, H. Ke, X. Zhao, and G. Xu, "Expected energy analysis for industrial process planning problem with fuzzy time parameters," *Computers and Chemical Engineering*, vol. 35, no. 12, pp. 2905–2912, 2011.

[30] B. Wang, G. D. Tian, Y. Liang, and T. G. Qiang, "Reliability modeling and evaluation of electric vehicle motor by using fault tree and extended stochastic Petri nets," *Journal of Applied Mathematics*, vol. 2014, Article ID 638013, 9 pages, 2014.